Agricultural and Forest Meteorology 232 (2017) 23–34

Contents lists available at ScienceDirect

Agricultural and Forest Meteorology

journal homepage: www.elsevier.com/locate/agrformet

Apparent winter CO_2 uptake by a boreal forest due to decoupling

Georg Jocher[a,*], Mikaell Ottosson Löfvenius[a,b], Giuseppe De Simon[b], Thomas Hörnlund[b], Sune Linder[c], Tomas Lundmark[a], John Marshall[a], Mats B. Nilsson[a], Torgny Näsholm[a], Lasse Tarvainen[a], Mats Öquist[a], Matthias Peichl[a]

[a] Swedish University of Agricultural Sciences (SLU), Department of Forest Ecology and Management, SE-901 83 Umeå, Sweden
[b] SLU, Vindeln Experimental Forests, SE-922 91 Vindeln, Sweden
[c] SLU, Southern Swedish Forest Research Centre, PO Box 49, SE-230 53 Alnarp, Sweden

ARTICLE INFO

Article history:
Received 25 January 2016
Received in revised form 3 August 2016
Accepted 5 August 2016

Keywords:
Advection
Coupling/decoupling
Eddy covariance
FLUXNET
Net ecosystem CO_2 exchange
Scots pine

ABSTRACT

Net uptake of carbon dioxide (CO_2) was observed during the winter when using the eddy covariance (EC) technique above a ~90-year-old Scots pine (*Pinus sylvestris* L.) stand in northern Sweden. This uptake occurred despite photosynthetic dormancy. This discrepancy led us to investigate the potential impact of decoupling of below- and above-canopy air mass flow and accompanying below-canopy horizontal advection on these measurements. We used the correlation of above- and below-canopy standard deviation of vertical wind speed (σ_w), derived from EC measurements above and below the canopy, as the main mixing criterion. We identified 0.33 m s^{-1} and 0.06 m s^{-1} as site-specific σ_w thresholds for above and below canopy, respectively, to reach the fully coupled state. Decoupling was observed in 45% of all cases during the measurement period (5.11.2014–25.2.2015). After filtering out decoupled periods the above-canopy mean winter NEE shifted from −0.52 μmol m^{-2} s^{-1} to a more reasonable positive value of 0.31 μmol m^{-2} s^{-1}. None of the above-canopy data filtering criteria we tested (i.e., friction velocity threshold; horizontal wind speed threshold; single-level σ_w threshold) ensured sufficient mixing. All missed critical periods that were detected only by the two-level filtering approach. Tower-surrounding topography induced a predominant below-canopy wind direction and consequent wind shear between above- and below-canopy air masses. These processes may foster decoupling and below-canopy removal of CO_2 rich air. To determine how broadly such a topographical influence might apply, we compared the topography surrounding our tower to that surrounding other forest flux sites worldwide. Medians of maximum elevation differences within 300 m and 1000 m around 110 FLUXNET forest EC towers were 24 m and 66 m, respectively, compared to 24 m and 114 m, respectively, at our site. Consequently, below-canopy flow may influence above-canopy NEE detections at many forested EC sites. Based on our findings we suggest below-canopy measurements as standard procedure at sites evaluating forest CO_2 budgets.

1. Introduction

Global warming, driven by the greenhouse gas concentrations in the atmosphere, affects the entire earth in manifold ways (e.g. IPCC, 2014). Forests play a crucial role in this context as they sequester carbon dioxide (CO_2) – a major greenhouse gas – all over the world. Consequently, confident predictions of both the future climate and forest carbon cycle require a thorough understanding and measurements of the processes determining the CO_2 sink strength of forest ecosystems.

The eddy covariance (EC) method has become the state-of-the-art method for quantifying the net ecosystem exchange (NEE) of CO_2 in various ecosystems all over the world. Around 40% of the 683 registered sites (as of April 2014) are classified as forest sites by FLUXNET, a worldwide network of EC flux measurement stations. The EC data are frequently used as the reference for compartmental fluxes of forest ecosystems and biometric measurements (e.g. Meyer et al., 2013; Peichl et al., 2010; Zha et al., 2007) or for validation of modeling approaches estimating gross primary production (GPP) and NEE (e.g. Beer et al., 2010; McCallum et al., 2013). Furthermore, EC data have been the basis for several high impact synthesis studies on global forest CO_2 sink strength (e.g. Beer et al., 2010; Fernández-Martínez et al., 2014; Keenan et al., 2013; Luyssaert et al., 2007; Mahecha et al., 2010; Schwalm et al., 2010). Misson et al. (2007) presented a synthesis study using EC data derived

* Corresponding author.
E-mail address: Georg.Jocher@slu.se (G. Jocher).

http://dx.doi.org/10.1016/j.agrformet.2016.08.002
0168-1923/

above and below the canopy at ten EC forest sites located in different climate zones worldwide. They stressed the importance of understory measurements for the interpretation of above canopy derived data. However, the clear majority of synthesis studies are based on single-level EC data derived above the forest ecosystem(s) without explicit analysis of the coupling behavior between below- and above-canopy air masses.

In a forest, the below-canopy airflow can be influenced by the local topography and thereby cause horizontal exchange of the below-canopy air (e.g. Belcher et al., 2012). For instance, local wind might flow preferentially downslope or upslope due to pressure gradients created in clear and calm weather situations (e.g. Butler et al., 2015; Kutsch and Kolari, 2015). The horizontal below-canopy flow needs special considerations in terms of data interpretation (e.g. Aubinet et al., 2005; Feigenwinter et al., 2004; Staebler and Fitzjarrald, 2004), especially if the vertical exchange between air masses below and above canopy is inhibited. Under such conditions the results based on above-forest measurements do not sufficiently reflect the whole ecosystem CO_2 exchange. Consequently, when decoupling and below-canopy horizontal flow occur there is potential for a considerable overestimation of the above-canopy derived forest CO_2 sink strength as below-canopy respiratory fluxes might not be detected at the EC system above canopy (Goulden et al., 1996).

During the last decades several studies have addressed theoretical issues regarding the complex energy and CO_2 exchange behavior in forests and between forest and atmosphere (e.g. Baldocchi and Meyers, 1988; Belcher et al., 2008; Finnigan, 2000; Fröhlich and Schmid, 2006; Launiainen et al., 2007; Lee, 2000; Raupach and Thom, 1981). Furthermore, a number of case studies have been published dealing with canopy decoupling and its carbon budget consequences for different sites and forest types. Feigenwinter et al. (2010), for instance, interpreted the CO_2 exchange of an alpine spruce forest in terms of a persistent local slope wind system. Vickers et al. (2012), Oliveira et al. (2013) and Alekseychik et al. (2013) investigated nocturnal sub-canopy horizontal flow regimes and their impact on above canopy CO_2 exchange during the growing season at their pine forest sites in Oregon (USA), southern Brazil and southern Finland, respectively. Nonetheless, even if the topic is not new, decoupling is still not considered at many EC forest sites. Most rely on above-canopy based descriptions of the coupling behavior, which may introduce a bias in the stand-scale CO_2 exchange estimates.

Currently, the most common filtering procedure to ensure good coupling is to use a friction velocity threshold derived from above-canopy EC measurements. The friction velocity threshold depends on canopy roughness, which in turn depends on site-specific quantities such as stem density, leaf area index and the vertical distribution of canopy foliar and branch biomass in the stand (e.g. Foken, 2008; Poggi et al., 2004). Nevertheless, in certain cases it might not be possible to determine a friction velocity threshold (e.g. chapter 5 in Aubinet et al., 2012) or it might not be sufficient to use such a threshold (e.g. Speckman et al., 2015).

The behavior of coherent structures of the flux of interest in the vertical column from soil to above canopy can also be used as an indicator of mixing (e.g. Foken et al., 2012; Serafimovich et al., 2011; Thomas and Foken, 2007). This method requires several EC measurements below, inside and above canopy and is therefore not affordable for most EC sites.

Another above-canopy variable for investigating the canopy-atmosphere mixing behavior is the standard deviation of the vertical wind velocity (e.g. Acevedo et al., 2009; Launiainen et al., 2005). Moreover, the relation of this variable between below- and above-canopy measurements can describe the coupling behavior: if air masses below and above canopy are fully coupled then this relation is linear (Thomas et al., 2013). This quality check is, however, not commonly used as it requires an additional EC system below the canopy.

Eddy covariance data from our site situated in northern Sweden indicate occurrences of net CO_2 uptake during winter periods. These observations are highly questionable since continuous gas exchange measurements in boreal Scots pine stands have shown that there was no net CO_2 uptake during the winter months November to February (e.g. Kolari et al., 2007; Linder and Lohammar, 1981; Troeng and Linder, 1982). Thus, some measurement artifact is highly likely. The biasing influence of decoupling and accompanying horizontal below-canopy air flow on the above-canopy derived NEE values has been shown for several forest types and stand densities during summer, both for daytime and nighttime conditions (e.g. Alekseychik et al., 2013; Thomas et al., 2013). An analysis of decoupling events during wintertime is, to our knowledge, currently lacking. Even if forest floor respiration is normally at a low rate during winter, it still contributes significantly to the annual ecosystem carbon budget (e.g. Goulden et al., 1998; Haei and Laudon, 2015; Ilvesniemi et al., 2005; Lindroth et al., 1998; Öquist and Laudon, 2008; Winston et al., 1997). Hence, decoupling and accompanying horizontal below-canopy flow may have an impact on the apparent carbon budget even during wintertime.

In this study, we analyzed a winter period (5.11.2014–25.2.2015) of NEE measurements above a boreal Scots pine forest and assessed coupling/decoupling and horizontal below-canopy flow. We used EC measurements below and above the canopy, following the approach proposed by Thomas et al. (2013). The overall aim was to examine to what extent decoupling and below-canopy horizontal flow were responsible for the observed negative NEE during winter despite the complete lack of photosynthesis during most of this period.

The main study objectives were:

i) to quantify the frequency of decoupling during wintertime.
ii) to investigate the potential implications of decoupling and horizontal below-canopy flow on the above-canopy derived NEE.
iii) to explore the potential of several filtering approaches for addressing coupling/decoupling, using quantities derived from above-canopy EC measurements.
iv) to compare the topography surrounding our EC tower to others in the worldwide network of forest flux sites (FLUXNET) as a means for determining how common such biased NEE results might be.

2. Materials and methods

2.1. Site description and characteristics

This study was conducted during the winter period of 5.11.2014–25.2.2015 at Rosinedalsheden experimental forest which is a ~90-year-old Scots pine (*Pinus sylvestris* L.) stand near Vindeln in northern Sweden (64°10′N, 19°45′ E; 155 – 160 m above sea level). The overall experiment was initiated in 2006 to study the effect of nitrogen (N) availability on stand-scale carbon cycling and consists of stands with high and low N addition rates, respectively, and a non-fertilized reference stand. Each stand is equipped with an EC tower for measuring the turbulent exchange of momentum, sensible heat, latent heat, and CO_2. The current study was conducted at the stand with the high N addition rate, which has received 100 and 50 kg N ha^{-1} yr^{-1} since 2006 and 2012, respectively, applied over an area of 15 ha around the EC tower.

The mean annual temperature in this region is 1.8 °C and the mean annual precipitation is 614 mm (Laudon et al., 2013; 30-year averages between 1981 and 2013 at the Svartberget field station, ca. 8 km away from the study site; www.slu.se/en/

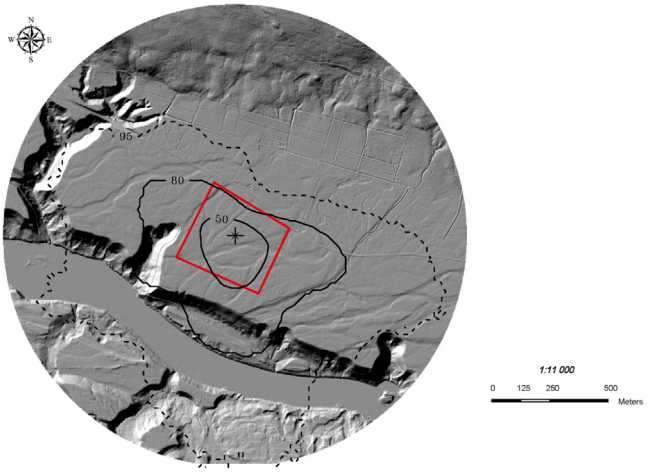

Fig. 1. Lidar derived digital elevation map (DEM) of the region of interest. The flux tower is marked by a black cross, the red rectangle shows the fertilized area. The additional lines with numbers in the figure mark the outer border of the areas, where in 50%, 80% and 95% of all cases the half-hourly flux values originate from (representative period 2.12.2014–15.12.2014). Calculation of footprint has been done with a lagrangian stochastic forward model, based on Rannik et al. (2000, 2003). (For interpretation of the references to color in this figure legend, the reader is referred to the web version of this article.)

departments/field-based-forest-research/experimental-forests/vindeln-experimental-forests/environmental-analysis/). Snow cover commonly occurs from early November to late April (Laudon and Ottosson Löfvenius, 2016) and the growing season usually lasts from early May to late September, following the growing season definition in Mäkelä et al., 2006 (cf. Lim et al., 2015), which is based on the behavior of snow cover and air temperature. Continuous shoot-level gas exchange measurements in the stand show that net photosynthesis is almost completely inhibited from the beginning of November until late March/early April (Göran Wallin, unpublished data). Consequently we assumed that photosynthesis was negligible for the winter period investigated in this study. The mean monthly temperatures below canopy during the investigation period (November 2014 to February 2015) were −1.5 °C, −3.2 °C, −3.3 °C and −3.3 °C, respectively.

Before the 2015 growing season, mean tree height at the study site was 17.3 m and the basal area 25.8 m^2 ha^{-1}. Maximum leaf area index in 2013 was ~3 m^2 m^{-2} (Lim et al., 2015). The sparse understory vegetation consists mainly of bilberry and cowberry (*Vaccinium myrtillus* L. and *Vaccinium vitis-idaea* L.), and a ground layer of mosses (Hasselquist et al., 2012).

The ground surface around the tower is rather flat up to a distance of ~200 m from the tower with a maximum elevation difference of ~2 m (Fig. 1). The maximum elevation differences within 300 m and 1000 m distance from the tower are 24 m and 114 m, respectively. These elevation differences are mainly caused by the deep river canyon southwest and a gentle slope northeast of the measurement site (Fig. 1). The footprint of fluxes above the canopy, calculated for a representative period with a lagrangian stochastic forward model based on Rannik et al. (2000, 2003), is also presented in Fig. 1.

2.2. Instrumentation

Flux data were obtained by two EC systems. The first system was installed above the forest at a height of 21.5 m and consisted of a Gill R3-100 (Gill Instruments Limited, Hampshire, UK) sonic anemometer for detecting wind components and sonic temperature and a LI-7200 (LI-COR Environmental, Lincoln, USA) gas analyzer for detecting H_2O and CO_2 mixing ratios. The second system (CPEC200 closed-path infrared gas analyzer combined with a CSAT3A sonic anemometer; Campbell Scientific, Logan, USA) measured the same quantities below the forest canopy at 2.5 m height and was located near the base of the high tower. Both systems sampled at a rate of 20 Hz. Before starting the experiment the two systems were compared by running them in parallel at the same height to ensure that there were no significant systematic differences in performance. The systems showed good agreement for best quality half-hourly data following the quality flagging scheme by Foken et al. (2004). A linear regression between the 30 min averages of vertical wind variances ($m\,s^{-1}$; key parameter for the considerations in this study) measured by the two systems (x = CPEC200, y = Gill/Li-7200) yielded a regression line slope of 1.04 and a zero intercept, suggesting a negligible bias. The comparison of the CO_2 concentration values provided by the two systems yielded a systematic deviation of ≈10 ppm (Gill/Li–7200 < CPEC200) which was accounted for the considerations in 2.4 and for Fig. 6.

2.3. Turbulent flux calculation

All vertical turbulent fluxes were calculated using the EC method (described in detail by e.g. Aubinet et al., 2012; Lee et al., 2004). Using this method vertical turbulent fluxes are derived from the covariance between the high frequency fluctuations of vertical wind and the quantity of interest (e.g. CO_2). Fluxes were calculated using TK3 which is a widely used EC software developed at the University of Bayreuth (Fratini and Mauder, 2014; Mauder and Foken, 2015). The TK3 software includes a quality flagging scheme which tests the data for stationarity and, if parameterizations of the stability-dependent integral turbulence characteristics are available for the quantity of interest, for development of turbulence. Turbulence is assessed by comparing the calculated and parameterized integral turbulence characteristics (Foken et al., 2004). However, similar to other EC software, it does not include any explicit test for detecting decoupling. In the subsequent analyses we used only the data flagged for best quality (class 1–3 according to Foken et al., 2004), exceptions are explicitly stated in the text.

2.4. Identification of coupled/decoupled periods

We used two parameters to identify decoupled periods: first we analyzed the correlation between the standard deviation of vertical wind velocity (σ_w) below vs. above the canopy. If the layers are coupled, σ_w for below and above canopy are linearly correlated (e.g. Thomas et al., 2013). We verified the threshold for σ_w above canopy following Thomas et al. (2013), considering the following correlation of above-canopy σ_w and above-canopy NEE: NEE ≈ constant if $\sigma_{w,abovecanopy} > \sigma_{w,threshold}$. The threshold for σ_w below canopy was determined by considering the correlation between below-canopy σ_w and the CO_2 concentration difference (ΔCO_2) between the below- and above-canopy EC system: $\Delta CO_2 \approx 0$ if $\sigma_{w,belowcanopy} > \sigma_{w,threshold}$.

Secondly, we used the wind directional shear between below and above canopy (vertical wind shear) to get additional insight into the coupling behavior. As we observed no distinct relation between vertical wind shear and above canopy NEE in our data set, we adopted the wind shear threshold between canopy middle and bottom that Alekseychik et al. (2013) used for a similar boreal pine forest site. Because the below-canopy flows were generally slow at our site, we added 10° and thus used 50° as wind shear threshold instead of the 40° used by Alekseychik et al. (2013). Additionally we assumed, according to Alekseychik et al. (2013), that wind directional shear is negligible above the middle and below the bottom of the canopy. In a parallel approach, we used above-canopy σ_w, friction velocity and horizontal wind speed to evaluate the feasibility

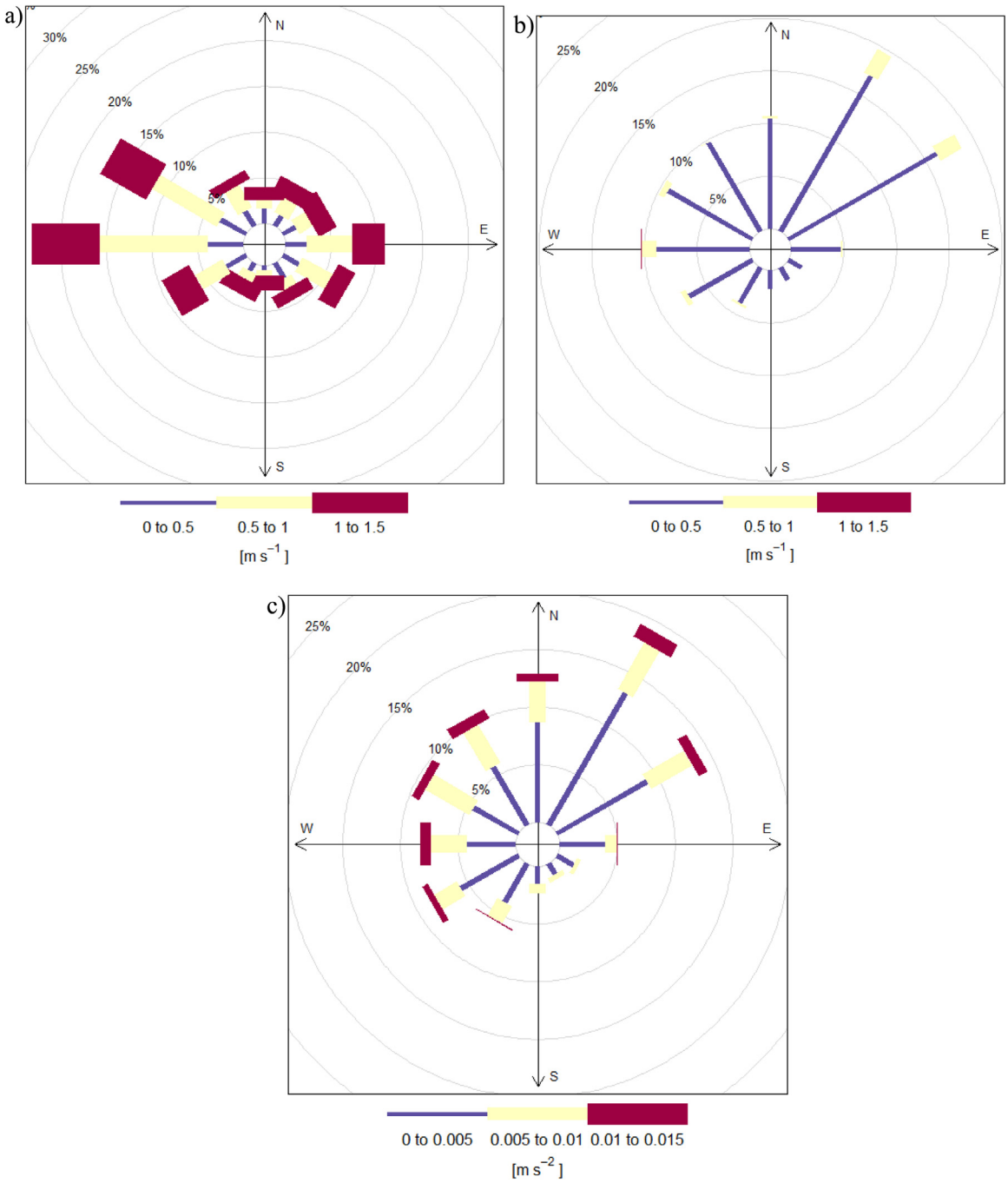

Fig. 2. Wind roses for above-canopy wind speed <1.5 m s^{-1} and Ri >0.25 conditions; a) above canopy, b) below canopy. In c) the buoyancy forcing (cf. Section 3.1) in dependency of wind direction below canopy is given for the same conditions as in a) and b).

of using above-canopy derived parameters as filter for decoupling events.

We also built a CO_2 flux benchmark data set by filtering all above-canopy derived CO_2 fluxes for quality and decoupling. We excluded all CO_2 flux values which did not have the best quality flag, leaving 30% of the initial data. We then filtered the remaining data ensuring that both σ_w below and above canopy were higher than the defined decoupling thresholds, which removed another 8% of the observations. In the end, 22% of the original above-canopy CO_2 flux measurements met these stringent criteria.

Furthermore, as additional information about atmospheric stability while investigating decoupling, we calculated the dimensionless Richardson number Ri (bulk version) across the air column between the below- and above-canopy EC systems according to Eq. (1). The Bulk Richardson number is an approach for the Gradient Richardson number, for which the critical Richardson number Ri_c is assumed to be approximately in the range from 0.21 to 0.25 (Stull, 1988). That means, that Richardson number values higher than Ri_c indicate suppressed turbulence and consequently stable atmospheric stratification. We used for the subsequent analysis a critical Richardson number of 0.25 which is in agreement with the Glossary of Meteorology of the American Meteorological Society (http://glossary.ametsoc.org/wiki/), even though several

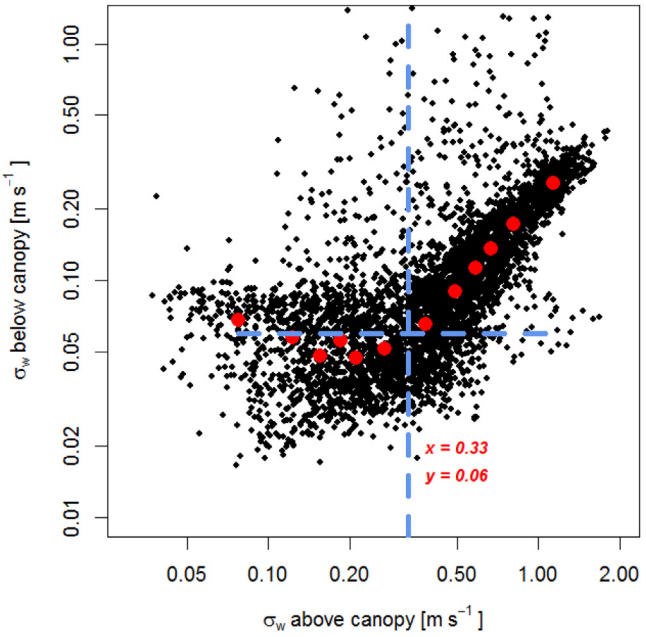

Fig. 3. Standard deviation of vertical wind velocity (σ_w) above canopy vs. σ_w below canopy ($m\,s^{-1}$) for the period 5.11.2014–25.2.2015, 30 min averages in black diamonds. The red filled circles represent median values of twelve binning classes of the 30 min σ_w averages. The crossing point of the two blue dashed lines marks the transition point from decoupling to coupling (relating coordinate values added in red). (For interpretation of the references to color in this figure legend, the reader is referred to the web version of this article.)

different recommendations to Ri_c exists in the literature (cf. e.g. Galperin et al., 2007).

$$Ri = \frac{g}{\overline{T}} \cdot \frac{\Delta\theta/\Delta z}{\left(\Delta u/\Delta z\right)^2} \quad (1)$$

In Eq. (1) g stands for the gravitational acceleration ($m\,s^{-2}$), T is the absolute temperature (mean across the layer of interest; K), the denominator of the second fraction describes the potential temperature gradient across the layer of interest and the nominator of this fraction the changes in horizontal wind speed across this layer. All needed quantities for Eq. (1) came from the two EC systems above and below canopy.

2.5. Estimating below-canopy respiration

As a first approach to estimate below-canopy respiration we applied Conditional Sampling on our unfiltered below-canopy EC data according to Eq. (2). Conditional Sampling, introduced by Desjardin (1977), is a modification of the EC method which assumes that the turbulent flux of the quantity of interest (here CO_2) can be derived by adding the separately determined flux components for positive (+; updraft) and negative (-; downdraft) vertical wind speeds w when the mean vertical wind speed is zero.

$$\overline{w'CO_2'} = \overline{w^+CO_2'} + \overline{w^-CO_2'} \quad (2)$$

Consequently, interested in the upward motion of CO_2 (≈respiratory flux), we estimated the below-canopy respiration flux using the first summand on the right side of Eq. (2) building the covariance (5 min averaging intervals) between CO_2 and vertical wind only for positive vertical wind speeds. The short averaging interval was chosen here to minimize potential instationarities caused by motions other than turbulence (cf. Thomas et al., 2013).

On top of the Conditional Sampling approach we estimated the below-canopy respiration using the below-canopy CO_2 flux data (30 min averages) which were processed as follows. Firstly, the 30 min below-canopy data had to fulfill the precondition of stationarity; for this we used the relating quality flag inherent in TK3. By doing this we justified the use of the 30 min averages as we could neglect a substantial change in the flux values between shorter covariances (5 min averages) and the final 30 min values in cases when stationarity can be assumed. Secondly, the σ_w values for decoupling for both measurement heights had to be below the thresholds for decoupling. Strongly coupled periods were thereby excluded as we were interested in estimating the amount of CO_2 resulting from below-canopy respiration that could be lost via horizontal advection during decoupled periods.

We cross-checked our EC derived estimates of below-canopy respiration with independent measurements of CO_2 diffusion through the snow pack based on snow pack CO_2 concentration gradients. The sample drawing and treating was identical to the procedure in Zhao et al. (2016), fluxes were calculated following Sommerfeld et al. (1993) and Seok et al. (2009). The measurements were conducted during the winters of 2011/2012 (n = 1; March 14)

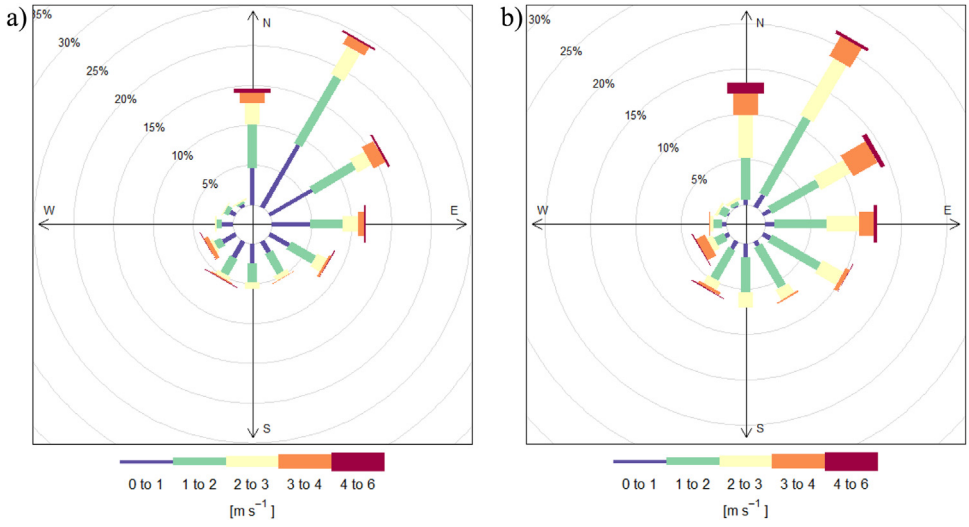

Fig. 4. Absolute value of wind shear (degree) between above and below canopy as a function of above canopy wind speed for a) all unfiltered data and b) all data after filtering for decoupling using the site specific σ_w thresholds (c.f. Section 3.2).

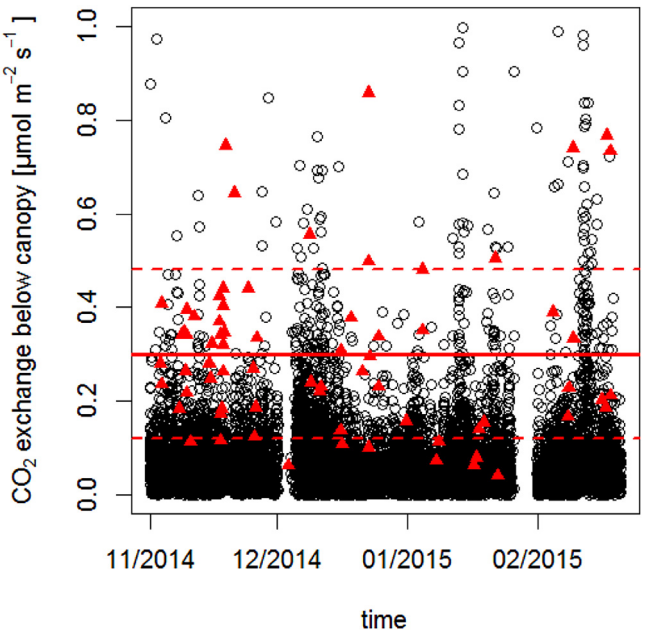

Fig. 5. The CO_2 exchange values (µmol m^{-2} s^{-1}) measured by the below-canopy EC system at 2.5 m and treated according to Section 2.5. The black circles indicate the Conditional Sampling results (5 min averages), the red triangles the output of TK3 (30 min averages). The red solid line denotes the mean CO_2 exchange of the 30 min averages, the dashed lines ± 1 SD. (For interpretation of the references to color in this figure legend, the reader is referred to the web version of this article.)

and 2012/2013 (n = 3; December 18, January 30, February 25). On each occasion samples were taken from six locations distributed in a 150 m long transect ca. 100 m west of the EC tower.

For subsequent analysis we refer mainly to the filtered EC 30 min. CO_2 exchange values as estimate of below-canopy respiration during winter and decoupling. Even though only ≈2% of data passed the stringent quality checks we assessed these data as the best possible estimate of below-canopy respiration due to the extensive filtering procedure. At these high latitudes the below-canopy respiration rates do not follow a significant diurnal radiation-induced temperature cycle during winter, mainly due to low insolation and the insulating effect of the snow covering the forest floor (e.g. Winston et al., 1997). Fig. A1 demonstrates that the below-canopy CO_2 exchange stayed nearly constant when global radiation reached values equal or higher than 20 W m^{-2} (which serves as a common global radiation threshold to separate between day and night conditions). Therefore, we considered this method as unlikely to result in large errors while extrapolating these few data for the entire observation period.

Having only a single measurement point below the canopy, we followed the approach by Thomas et al. (2013) for assumptions about below-canopy horizontal advection. In this approach the below-canopy respiration equals to below-canopy horizontal advection during decoupling.

2.6. Investigating the influence of topography at FLUXNET sites worldwide

To determine whether decoupling and horizontal advection were especially severe at our site due to a more variable topography than at forest EC sites worldwide we examined all registered FLUXNET forest sites. The final selection included sites with an accuracy in their coordinates of at least five digits (coordinate information obtained in summer 2015 via www.fluxdata.org; n = 110). For these sites, we determined the maximum elevation differences around each tower within a radius of 300 m and 1000 m, respectively, using information from the U.S. Geological Survey (www.usgs.gov; Shuttle Radar Topography Mission (SRTM) data, reference height system: World Geodetic System 1984; access: summer 2015). Due to their better resolution we used Swedish and Finnish land surveying data (www.lantmateriet.se and www.maanmittauslaitos.fi) to obtain this information for Swedish and Finnish sites.

3. Results and discussion

3.1. Vertical wind shear across the canopy layer

Using a vertical wind shear threshold of 40° (separate from the decoupling threshold), we found that 64% of the whole measurement period was accompanied by vertical wind shear. Furthermore, we detected a dominant below-canopy wind direction from the north-east, which most likely reflects the influence of tower-surrounding topography. Given the steep slope in the south and west around 250 m away from the measurement tower and a

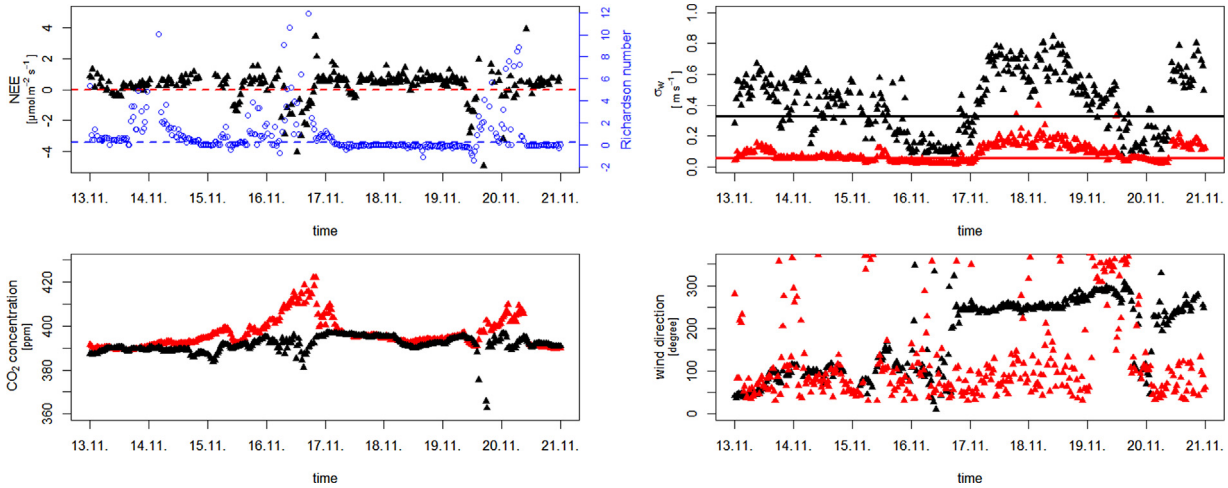

Fig. 6. Above-canopy NEE (µmol m^{-2} s^{-1}) and Richardson numbers (blue; both upper left panel), CO_2 concentration (ppm; lower left panel) above (black) and below (red) canopy, σ_w (m s^{-1}; upper right panel) above (black) and below (red) canopy and wind direction (degree; lower right panel) above (black) and below (red) canopy for a 8-days example period in November 2014. The red dashed line in the upper left panel is a zero line, the blue dashed line in the same panel marks the critical Richardson number 0.25. The black and red horizontal lines in the upper right panel marks the σ_w thresholds for decoupling as defined in Section 3.2. (For interpretation of the references to color in this figure legend, the reader is referred to the web version of this article.)

gentle slope in the northeast around 600 m away (cf. Fig. 1), flow from northeast (downslope) might be expected. To visualize and demonstrate the effect of wind shear and predominant below-canopy flow direction Fig. 2 shows wind roses for relatively calm wind conditions (above-canopy horizontal wind <1.5 m s^{-1}) and stable stratification according to the Richardson number results (Ri >0.25). The strength of this feature gradually decreased with rising above-canopy wind speed and vanished when the horizontal wind speed above canopy exceeded a threshold of around 4 m s^{-1} (not shown here). Above- and below-canopy wind directions converged then due to enhanced mechanical turbulent mixing, the flow characteristics at these two layers got synchronized.

An appropriate quantity to check whether an observed preferential below-canopy flow might be topographically induced is the buoyancy forcing. Negative buoyancy forcing associated with preferential flow directions near the ground are a clear hint for topographically induced drainage flow (cf. Staebler and Fitzjarrald, 2005). We calculated the buoyancy forcing using Eq. (1) without the wind gradient (i.e. buoyancy forcing = $-(g/\overline{T} \cdot \Delta\theta/\Delta z)$). Fig. 2c) shows the buoyancy forcing in dependency of below-canopy wind direction for the same conditions as in Fig. 2a) and Fig. 2b). Clearly visible is the preferential wind sector from northeast (≈30°) for negative buoyancy forcing, the largest fraction of high absolute numbers of negative buoyancy forcing are also evident during flow from this sector. The tower-surrounding terrain is rising (from the tower's perspective) in direction 30° for roughly 1300 m with a mean inclination of ≈6.3°. Consequently, these findings confirm the assumption that the observed preferential below-canopy flow is most likely, to a great extent, topographically induced by the gentle slope in the northeast of our measurement tower.

Additionally it got obvious, that the above-canopy wind field by itself (and therefore the wind shear between below and above canopy) is also influenced by the tower surrounding topography to some extent. Comparing the above-canopy wind field with independent wind field measurements at the Svartberget reference climate station (at 38 m height, about 16 m above a spruce forest) revealed that channeling and shading effects might apply at the EC system above canopy (Fig. A2). The wind field at the EC system above canopy shows a more pronounced west-east orientation (likely channeling along the river valley; cf. Fig. 1) and less wind from the sector between north and east (potential shading effect of elevations north of the EC tower) than the wind field during the same period at Svartberget.

3.2. Standard deviation of vertical wind velocity below and above canopy

The linear correlation between σ_w below and above the canopy broke down at thresholds of less than 0.06 m s^{-1} and 0.33 m s^{-1} below and above canopy, respectively (Fig. 3; R^2 = 0.56 for the data range above the thresholds). The mixing of air masses through the canopy depends on the site-specific canopy roughness, which is determined by forest properties like tree height, stem density, leaf area index, and crown density (cf. e.g. Aubinet et al., 2012). Consequently, other authors have reported slightly different σ_w thresholds, e.g., 0.10 and 0.43 m s^{-1} during nighttime in summer for a Scots pine stand in Hyytiälä, Finland (Alekseychik et al., 2013). In addition to the roughness dependency this thresholds may also vary with the time of the day, especially during the summer. During the day, turbulence and mixing are more pronounced. Thomas et al. (2013) discriminated between day and night in their analysis of the coupling/decoupling behavior during summertime at a Douglas-fir site in Oregon. We did not separate between day and night in our data analysis as the winter daylight period is short (i.e. 4–6 h) and temperatures are continuously low at these high latitudes.

Moreover, when above-canopy turbulence is very weak (low σ_w values above canopy), below-canopy turbulence can increase due to greater vertical wind directional shear (Fig. 3; cf. Thomas et al., 2013).

3.3. Periods of decoupled canopy: quantification

As defined in the previous section, all periods with σ_w < 0.06 m s^{-1} for the below-canopy system and σ_w < 0.33 m s^{-1} above canopy were considered as decoupled. On this filtered data set a vertical wind shear of more than 50° was applied as supplementary decoupling indicator.

Filtering the original untreated data only with the above mentioned thresholds for σ_w excluded around 45% of all data. Including vertical wind shear as an additional filter excluded around 65% of the data. Consequently, the two filtering criteria (wind shear and σ_w thresholds) did not exclude the same data populations. As can be seen in Fig. 4a) and b), vertical wind shear still existed to some extent even if the air masses below and above canopy were fully coupled according to the derived σ_w thresholds. Furthermore, higher wind speeds above canopy coincided with damped vertical wind shear (Fig. 4a & b).

Several different layers of wind directional shear could develop along the vertical column from the ground surface to a few meters above the canopy (e.g. Alekseychik et al., 2013). Hence, investigating vertical wind shear in and above forest canopies with only two measurement heights may not be sufficient to fully account for the problem.

3.4. Implications of decoupling on the forest carbon budget

The below-canopy CO_2 exchange measurements were mostly positive and indicated that respiration exceeded photosynthesis, as expected. The mean below-canopy CO_2 exchange was estimated to be in the range from 0.07 ± 0.06 (average ± SD; Conditional Sampling with 5 min averages) to 0.30 ± 0.18 (average ± SD; 30 min values) μmol m^{-2} s^{-1} (Fig. 5). Independent measurements of CO_2 diffusion through the snowpack sporadically conducted in previous winters yielded an average winter soil respiration rate of 0.14 ± 0.06 (average ± SD) μmol m^{-2} s^{-1}. These diffusion estimates confirm our EC derived 30. min. results, considering the larger footprint and hence expectable higher fluxes at the EC system below canopy. Consequently, for the following discussion the 30 min values will be used. Additionally, we considered our EC based 30 min results as a lower limit of respiratory flux at below-canopy EC system measurement height as the measured below-canopy CO_2 exchange is not necessarily equal to below-canopy respiration in the absence of photosynthesis due to the potential influence of downward drafts of air parcels in the decoupled below-canopy layer (cf. Thomas et al., 2013). These downward drafts may bias the measured flux in negative direction. However, using only data with best quality flags (i.e. well-developed turbulence, c.f. Section 2.5) for the estimation of below-canopy CO_2 exchange during decoupling should minimize this effect. Integrating the below-canopy CO_2 exchange over the whole investigated winter period suggested a total emission from the forest floor of 126 ± 76 g CO_2 m^{-2} (34 ± 21 g C m^{-2}). Decoupling occurred during 45% of this period when using only σ_w thresholds and during 65% of the time with vertical wind directional shear was as an additional decoupling indicator. In a worst-case scenario, i.e. assuming perfect decoupling and 100% advective loss of the below-canopy air mass, those decoupled periods would amount to a total of 57 ± 34 (for using only the σ_w thresholds) and 80 ± 48 (σ_w thresholds combined with wind shear threshold) g CO_2 m^{-2} (15.6 ± 9.3 and 21.8 ± 13.1 g C m^{-2}), respectively, not being captured with the above-canopy measurements. This carbon loss would have a significant impact on the

estimated forest ecosystem carbon budget. For instance, previous studies on annual boreal pine forest carbon budgets, using only above-canopy measurements, report annual EC NEE values ranging from 136 to 241 g C m^{-2} uptake for a ~45-year-old Scots pine forest (Kolari et al., 2009) and up to 323 g C m^{-2} uptake for a ~75-year-old Scots pine plantation (Kolari et al., 2004). Suni et al. (2003) reported uptake values from 162 to 307 g C m^{-2} y^{-1} for a ~80-year-old boreal Scots pine stand. Thus, our results suggest that the seasonal and consequently annual ecosystem-scale carbon sink strengths might be considerably overestimated when not accounting for the below-canopy carbon loss.

The above carbon loss estimates are upper limits on the potential influence of decoupling and below-canopy horizontal advection on above-canopy derived NEE. There might be other processes that transport accumulated below-canopy CO_2 after decoupled periods up to the EC system above canopy. Furthermore, air masses which left the relevant below-canopy footprint could be transported back as well. Thomas et al. (2013) give more information on potential shortcomings of their approach to address decoupling and below-canopy horizontal advection.

3.5. Applicability of above-canopy derived parameters for identifying decoupling

Given that a large number of EC forest sites worldwide rely only on above-canopy measurements, a crucial question is whether any parameter available from above-canopy measurements might serve as a robust indicator for detecting decoupled conditions. The availability of such a parameter would furthermore offer the opportunity to correct historical data for the potential bias in above-canopy derived NEE values due to decoupling processes.

In our study, above-canopy net ecosystem CO_2 exchange (NEE) for the fully coupled periods was 0.31 ± 0.19 μmol m^{-2} s^{-1}. This is slightly lower but comparable with a previously reported value of 0.44 μmol m^{-2} s^{-1} for winter ecosystem respiration at a ~40-year-old Scots pine stand in Southern Finland (Markkanen et al., 2001) with a leaf area index of 9 m^2 m^{-2} (all-sided). We set u_* and horizontal wind speed thresholds such that the proportions of the data that were filtered were equal to those in the benchmark decoupling dataset. This yielded an u_* threshold of 0.26 m s^{-1} and a horizontal wind speed threshold of 1.13 m s^{-1}. However, these two data populations matched the benchmark population in only to 81% and 76% of data points, respectively, indicating that the u_* and wind speed filtering did not identify all decoupled periods. Filtering the initial NEE values with only the above-canopy σ_w threshold yielded a 90% match with the benchmark data population. All three single-level above-canopy filtering methods resulted in less positive estimates of mean NEE (±SD) in comparison to the benchmark data set, namely 0.13 ± 0.20 μmol m^{-2} s^{-1} for u_* filtering, 0.10 ± 0.20 μmol m^{-2} s^{-1} for wind speed filtering, and 0.14 ± 0.20 μmol m^{-2} s^{-1} for single-level σ_w filtering (Table 1). This indicates clearly that, even if there is a match of up to 90% between the single-level and two-level filtered data populations, a single-level filtering with above-canopy derived data might not be sufficient to fully address the effects of decoupling and below-canopy horizontal flow. The difference in the data captured by the single-level filtering vs. the two-level filtering had a severe influence on the above canopy derived NEE. A reliable method is needed to reduce the potential bias in ecosystem-scale CO_2 flux estimates due to below-canopy fluxes not being captured in above-canopy NEE measurements during decoupled conditions. Eddy covariance measurements below the forest canopy can provide a remarkable improvement here.

3.6. Apparent winter CO_2 uptake due to decoupling

The photosynthetic apparatus is not always inactive during winter in boreal forests. Short periods of net CO_2 uptake do occur on mild days (e.g. Troeng and Linder, 1982) even if the photosynthetic efficiency is low (Kolari et al., 2007; Strand and Öquist, 1985). However, long-term means should not show negative NEE fluxes, i.e. net CO_2 uptake by the forest, during winter, as suggested by our unfiltered EC measurements. This result contrasts with long-term gas exchange measurements in boreal Scots pine forests (cf. Kolari et al., 2007; Troeng and Linder, 1982).

Fig. 6 visualizes a 8-days example period showing the unfiltered NEE above canopy and the corresponding Richardson numbers (upper left panel), the CO_2 concentration patterns below and above canopy (lower left panel) and wind characteristics (σ_w and direction) below and above canopy (right panels). Between November 16 and 17 and later mid of November 19 uptake above the canopy is visible. This is associated with stable stratification ($Ri > 0.25$), decoupling according to the σ_w thresholds and a temporary accumulation of CO_2 below the canopy. Obviously, decoupling events take place here which leads to CO_2 accumulation below the canopy and a bias in the above-canopy NEE. Stable stratification is a precondition for such an event, but Fig. 6 also shows that stable stratification alone does not always lead to a bias in the above-canopy NEE (see the data around 14.11. in Fig. 6 where, according to the σ_w thresholds, no decoupling but stable stratification occurs). Interestingly, the ends of the decoupling events and CO_2 accumulation below canopy coincide with a rapid change in above-canopy wind direction and consequently pronounced wind shear between below and above canopy. This feature might be an example of increased mixing produced by wind shear between below and above canopy as it is e.g. reported in Thomas et al. (2013). While with better mixing the NEE quickly returns to positive values stays below-canopy wind direction constant. Possibly, parts of the accumulated CO_2 are then horizontally transported away via this below-canopy flow. Overall, a bias of NEE in negative direction is clear to see as the apparent uptake is not fully compensated by corresponding positive values after the decoupling events.

Considering the randomness of turbulence and winter NEE values near zero, we expected to still observe some negative NEE values in our benchmark data set. The percentage of negative NEE values in our wintertime data declined from 48% for the unfiltered fluxes to 41% for best quality data to 35% for the benchmark data set, which was filtered for quality and decoupling. Furthermore, the mean NEE shifted from negative (CO_2 uptake) to positive (CO_2 emission) values with increasing strictness of data filtering, the frequency and magnitude of high and low instantaneous NEE values declined as well (Fig. 7). It is noteworthy that most of the remaining negative NEE values were obtained during periods when the wind originated from north (wind direction ~<90° or wind direction ~>270°) while south winds yielded more positive NEE values (Fig. 7). This may demonstrate the influence of topography on data, even when they were filtered for quality and decoupling events. Wind from northern directions is flowing downslope following the local topography (cf. Fig. 1) and arrives at the sonic anemometer with a vertical angle different from zero, which can mimic a negative (downward) flux. Effects like this should have been excluded by the coordinate rotation done in the normal course of the turbulent flux calculations. Still, there might be a small topographical influence on the flux results due to an imperfection in the coordinate rotation. Especially in complex, forested terrain flux calculations can be influenced by such issues (e.g. Ross and Grant, 2015).

Table 1
Performance of different parameters for above-canopy EC NEE filtering regarding coupling/decoupling compared to completely untreated data and a benchmark data set.

	Critical value (m s^{-1})§	Matching with benchmark data set£	Mean NEE (μmol m^{-2} s^{-1})$
Untreated	–	–	*−0.52 ± 2.10*
Benchmark	–	*100%*	*0.31 ± 0.19*
SD vertical wind	0.33	90%	0.14 ± 0.20
Friction velocity	0.26	81%	0.13 ± 0.20
Horizontal wind	1.13	76%	0.10 ± 0.20

§ – required filter values to get the same amount of data points as the benchmark data set has.
£ – benchmark: above canopy NEE with best quality for fully coupled periods using a two-level filtering (cf. Section 2.4).
$ – mean NEE for data sets based on varying selection criteria.

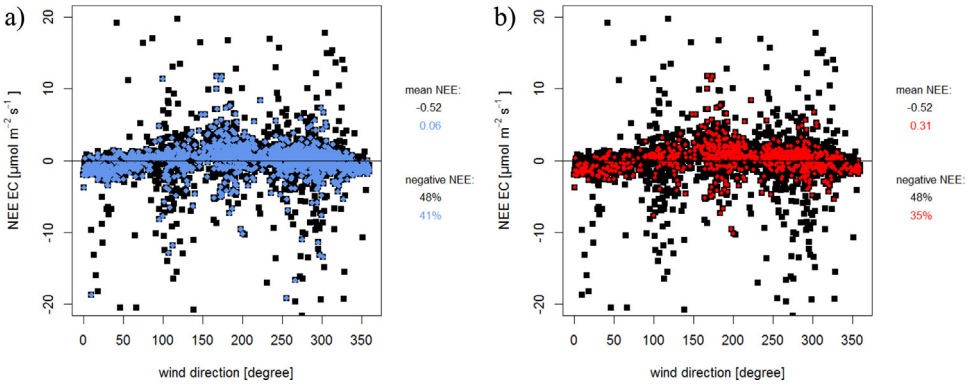

Fig. 7. Wind direction (degree) above canopy vs. NEE (μmol m^{-2} s^{-1}) above canopy. Unfiltered flux results are shown in black, data with best quality considering all coupling stages in blue (a) and data with best quality only for fully coupled periods (benchmark data set) in red (b). With strictness of data filtering, the percentage part of negative NEE decreases and the mean NEE shifts from negative to positive values (color-coded shown on the right part of the panels). (For interpretation of the references to color in this figure legend, the reader is referred to the web version of this article.)

3.7. Global relevance of decoupling and below-canopy horizontal advection

Given the roughness of forest canopies (e.g. Poggi et al., 2004) decoupling may occur at the majority of forested EC measurement sites around the world. When decoupling coincides with sloping terrain horizontal advection below the canopy can be fostered.

As introduced in 2.1, the topography surrounding the tower at our site is rather flat with a maximum elevation difference of 2 m within a distance of ~200 m from the tower. Beyond 200 m, the maximum elevation differences are 24 m and 114 m within 300 m and 1000 m, respectively, and a severe influence of topography was reflected by a predominant wind direction below the canopy (Fig. 2). This raises the question of how general such features may be. We therefore compared the topography at our site to that of 110 forest FLUXNET sites (cf. Section 2.6). Medians of maximum elevation differences in a circle around these towers, with a radius of 300 m or 1000 m, were 24 m and 66 m, respectively (Fig. 8). These results indicate that hilly topography within such distances is a common feature which likely affects EC derived forest carbon budget estimations at many forested EC sites worldwide.

However, a potential influence of topographically induced below-canopy horizontal flow on the above canopy derived NEE values has to be evaluated for each site separately. Vickers et al. (2012) suggested that a conventional filtering of above-canopy derived summertime flux data at a certain friction velocity threshold is sufficient for addressing the coupling/decoupling issue at their site. This study was conducted at a mature ponderosa pine forest in Oregon with canopy height 10–16 m and leaf area index 3.1–3.3 m^2 m^{-2}, situated on a flat saddle (~500 × 500 m) surrounded by complex terrain. The maximum elevation differences within a 300 m and 1000 m radius around the measurement tower at this site were 14 m and 88 m, respectively, and therefore lower than the corresponding values for our site (24 m and 114 m). In contrast, a relatively high friction velocity threshold (Speckman et al., 2015) could not solve the disagreement between EC derived summertime carbon fluxes and compartmental estimates of the carbon budget at the GLEES Ameriflux site. This site is characterized by a mixed spruce and subalpine fir stand with 18 m mean tree height. It is situated in high elevated, steeply sloping, mountainous terrain with maximum elevation differences of 68 m and 148 m, respectively, within 300 m and 1000 m radius around the measurement tower. These elevation differences are considerably higher than at our site. Even when the leaf area index decreased from around 6.1 m^2 m^{-2} to 0.9 m^2 m^{-2} after a massive bark beetle infection, a disagreement still existed. The steep terrain at the GLEES Ameriflux site might be a key factor in these difficulties. However, as we are lacking in more detailed information for both the above sites, we can only speculate for now.

As previously mentioned, the use of a friction velocity threshold has been established as the most accepted and widely used approach to address the problem of inadequate turbulent mixing in forest EC studies (e.g. Fernández-Martínez et al., 2015; Morgenstern et al., 2004; Vickers et al., 2012). However, a growing number of studies are strongly questioning the effectiveness of using only a friction velocity threshold derived from above-canopy measurements (e.g. Acevedo et al., 2009; Kutsch and Kolari, 2015; Speckman et al., 2015; Thomas et al., 2013). Furthermore, just recently underlined by Kutsch and Kolari (2015), it is getting more and more obvious that including a detailed analysis of the potential influence of surrounding topography on above-canopy derived EC results is of prime importance. Even though this topic is still intensely debated and a general agreement has yet to be achieved, our study further supports the call for a better understanding of above- and below-canopy exchange dynamics and of the influence of topography surrounding EC towers on above-canopy derived EC measurements. Such knowledge will be crucial to improve estimates of the CO_2 sink-source strength of forest ecosystems worldwide.

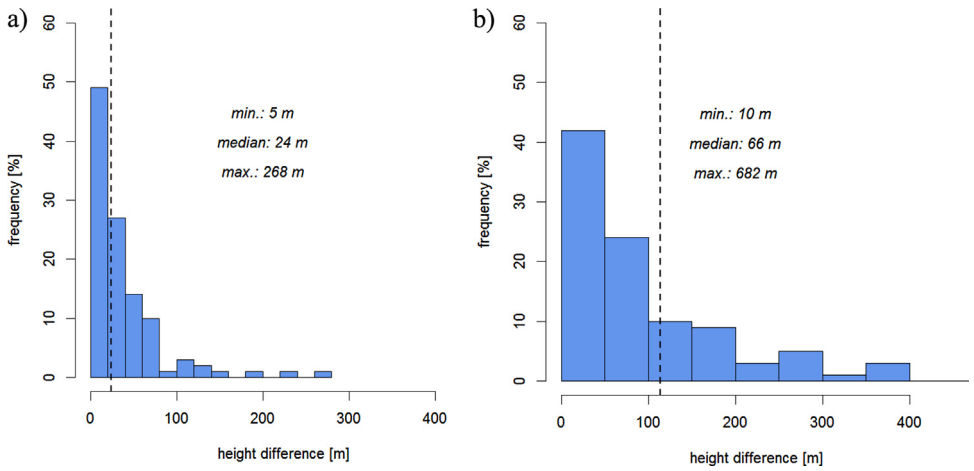

Fig. 8. Maximum height difference between tower base and any point within a circular area with a radius of a) 300 m and b) 1000 m. Shown are selected FLUXNET forest sites (n = 110, see Section 2.6 for details). The vertical dashed lines mark the corresponding values for the measurement site presented in this paper.

4. Conclusions

Apparent CO_2 uptake in above-canopy winter EC CO_2 fluxes led us to investigate the decoupling between above- and below-canopy air masses and potential accompanying below-canopy horizontal advection. We found that decoupling occurs frequently in this boreal forest despite a low leaf area index and that tower-surrounding topographical features are able to foster below-canopy drainage flow even when the nearest vicinity around the measurement tower is rather flat. Both decoupling and below-canopy horizontal drainage flow may promote below-canopy advective CO_2 loss. Even in wintertime when CO_2 fluxes are very low at these high latitudes, this potential advective carbon loss may account for a substantial part of the whole forest seasonal and, therefore, annual carbon budget.

We evaluated three different parameters derived from above-canopy measurements for their usefulness for identifying periods with decoupling. Neither a filtering with an above-canopy derived u_* threshold, nor a horizontal wind speed threshold, nor a filtering with an above-canopy derived σ_w threshold could reproduce the above-canopy CO_2 flux data filtered with σ_w thresholds for both above- and below-canopy data.

Based on these findings we conclude that: (i) decoupling may occur even in quite open forest stands; (ii) filtering flux data with single-level above-canopy derived parameters is not a sufficient alternative for two-level investigations to address decoupling; (iii) topography beyond the nearest vicinity to the flux tower might have a profound influence on the EC measurements.

Moreover, the maximum elevation differences around 110 forest FLUXNET sites within an area of 300 m and 1000 m distance to the towers showed clearly that the topography at our site is not unusual; most of the forest EC towers are measuring CO_2 fluxes over topography that is similar or characterized by even greater elevation differences than at our site. This indicates a potential for the influence of decoupling and below-canopy horizontal flow at many forested sites worldwide. We therefore recommend that additional below-canopy measurements should be included as standard procedure for measuring the forest CO_2 balance worldwide.

Conflicts of interest

The authors declare that there are no conflicts of interest regarding the publication of this paper.

Acknowledgments

The Rosinedalsheden research site was established with support from the Kempe Foundations and the Swedish Research Council for Environment, Agricultural Sciences and Spatial Planning (FORMAS) and is since 2014 part of the "*Swedish Infrastructure for Ecosystem Science*" (SITES) funded by the Swedish Research Council (VR) and partner universities. This study received support from the research programs "Future Forests" (Swedish Foundation for Strategic Environmental Research – MISTRA), "Trees and Crops for the Future" (Swedish Governmental Agency for Innovation Systems – VINNOVA) and "Nitrogen and Carbon in Forests" (FORMAS). Furthermore, the scholarship from Kempe Foundations to Georg Jocher is gratefully acknowledged.

Appendix A.

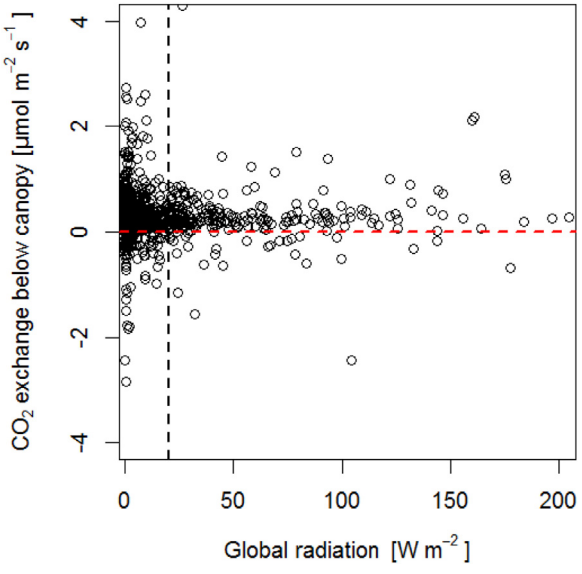

Fig. A1. CO_2 exchange below canopy ($\mu mol\ m^{-2}\ s^{-1}$; unfiltered EC derived 30 min averages) in dependency of global radiation ($W\ m^{-2}$; measured at Svartberget Forest research station). The red dashed horizontal line marks the zero line, the black dashed vertical line marks the used global radiation threshold to separate between day and night conditions ($20\ W\ m^{-2}$). (For interpretation of the references to colour in this figure legend, the reader is referred to the web version of this article.)

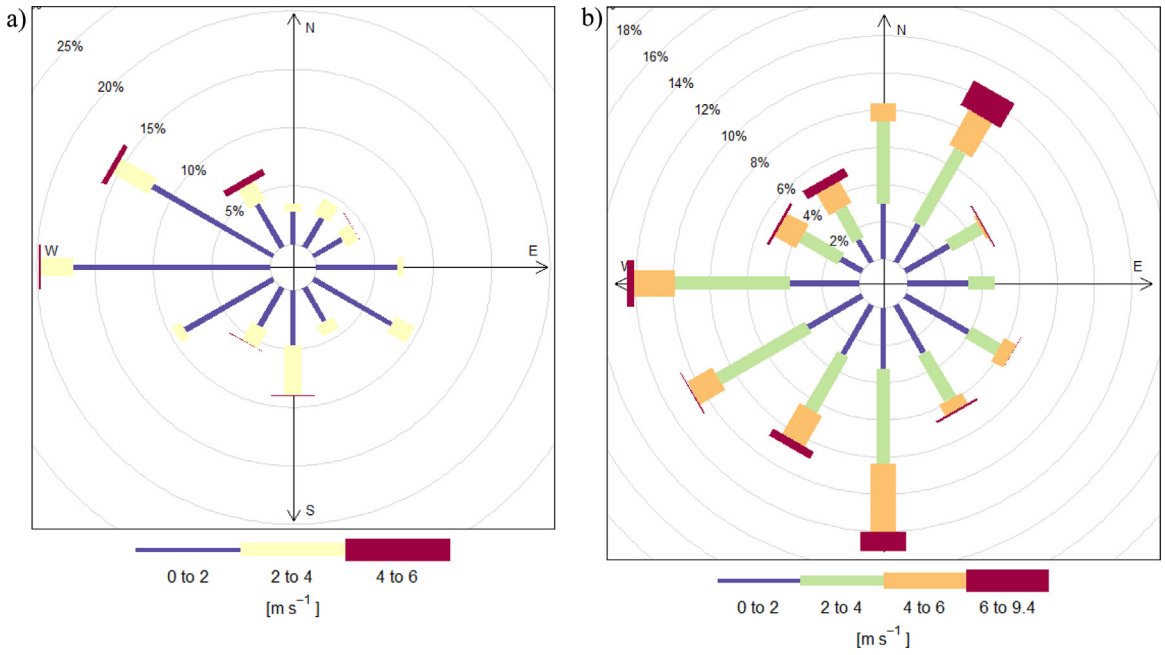

Fig. A2. a) Wind rose built with all available wind data of the EC system above canopy. b) Reference wind rose derived from propeller anemometer data (38 m above ground, around 16 m above spruce forest) at the Svartberget reference climate station.

References

Öquist, M.G., Laudon, H., 2008. Winter soil-frost conditions in boreal forests control growing season soil CO_2 concentration and its atmospheric exchange. Global Change Biol. 14, 1–9.

Acevedo, O.C., Moraes, O.L.L., Degrazia, G.A., Fitzjarrald, R.D., Manzi, A.O., Campos, J.G., 2009. Is friction velocity the most appropriate scale for correcting nocturnal carbon dioxide fluxes? Agric. For. Meteorol. 149, 1–10.

Alekseychik, P., Mammarella, I., Launiainen, S., Rannik, Ü., Vesala, T., 2013. Evolution of the nocturnal decoupled layer in a pine forest canopy. Agric. For. Meteorol. 174–175, 15–27.

Aubinet, M., Berbigier, P., Bernhofer, C.H., Cescatti, A., Feigenwinter, C., Granier, A., Grunwald, T.H., Havrankova, K., Heinesch, B., Longdoz, B., Marcolla, B., Montagnani, L., Sedlak, P., 2005. Comparing CO_2 storage and advection conditions at night at different carboeuroflux sites. Boundary Layer Meteorol. 116, 63–94.

Aubinet, M., Feigenwinter, C., Heinesch, B., Laffineur, Q., Papale, D., Reichstein, M., Rinne, J., van Gorsel, E., 2012. Nighttime flux correction. In: Aubinet, M., Vesala, T., Papale, D. (Eds.), Eddy Covariance: A Practical Guide to Measurement and Data Analysis. Springer, Dordrecht/Heidelberg/London/New York, pp. 133–157.

Baldocchi, D.D., Meyers, T.P., 1988. Turbulence structure in a deciduous forest. Boundary Layer Meteorol. 43, 345–364.

Beer, C., Reichstein, M., Tomelleri, E., Ciais, P., Jung, M., Carvalhais, N., Rödenbeck, C., Altaf Arain, M., Baldocchi, D., Bonan, G.B., Bondeau, A., Cescatti, A., Lasslopp, G., Lindroth, A., Lomas, M., Luyssaert, S., Margolis, H., Oleson, K.W., Roupsard, O., Veenendaal, E., Viovy, N., Williams, C., Woodward, F.I., Papale, D., 2010. Terrestrial gross carbon dioxide uptake: global distribution and covariation with climate. Science 329, 834–838.

Belcher, S.E., Finnigan, J.J., Harman, I.N., 2008. Flows through forest canopies in complex terrain. Ecol. Appl. 18, 1436–1453.

Belcher, S.E., Harman, I.N., Finnigan, J.J., 2012. The wind in the willows: flows in forest canopies in complex terrain. Annu. Rev. Fluid Mech. 44, 479–504.

Butler, B.W., Wagenbrenner, N.S., Forthofer, J.M., Lamb, B.K., Shannon, K.S., Finn, D., Eckman, R.M., Clawson, K., Bradshaw, L., Sopko, P., Beard, S., Jimenez, D., Wold, C., Vosburgh, M., 2015. High-resolution observations of the near-surface wind field over an isolated mountain and in a steep river canyon. Atmos. Chem. Phys. 15, 3785–3801.

Desjardin, R.L., 1977. Description and evaluation of a sensible heat flux detector. Boundary Layer Meteorol. 11, 147–154.

Feigenwinter, C., Bernhofer, C., Vogt, R., 2004. The influence of advection on the short term CO_2-budget in and above a forest canopy. Boundary Layer Meteorol. 113, 201–224.

Feigenwinter, C., Montagnani, L., Aubinet, M., 2010. Plot-scale vertical and horizontal transport of CO_2 modified by a persistent slope wind system in and above an alpine forest. Agric. For. Meteorol. 150, 665–673.

Fernández-Martínez, M., Vicca, S., Janssens, I.A., Sardans, J., Luyssaert, S., Campioli, M., Chapin, F.S., Ciais, P., Malhi, Y., Obersteiner, M., Papale, D., Piao, S.L., Reichstein, M., Rodà, F., Peñuelas, J., 2014. Nutrient availability as the key regulator of global forest carbon balance. Nat. Clim. Change 4, 471–476.

Fernández-Martínez, M., Vicca, S., Janssens, I.A., Sardans, J., Luyssaert, S., Campioli, M., Chapin, F.S., Ciais, P., Malhi, Y., Obersteiner, M., Papale, D., Piao, S.L., Reichstein, M., Rodà, F., Peñuelas, J., 2015. Response to: Kutsch, W.L, Kolari, P., 2015. Data quality and the role of nutrients in forest carbon-use efficiency. Nature Climate Change 5, 959–960. Nat. Clim. Change 5, 960–961.

Finnigan, J., 2000. Turbulence in plant canopies. Annu. Rev. Fluid Mech. 32, 519–571.

Foken, T., Göckede, M., Mauder, M., Mahrt, L., Amiro, B.D., Munger, W.J., 2004. Post-field data quality control. In: Lee, X., Massmann, W.J., Law, B. (Eds.), Handbook of Micrometeorology: A Guide for Surface Flux Measurements and Analysis. Kluwer, Dordrecht, pp. 181–208.

Foken, T., Meixner, F.X., Falge, E., Zetzsch, C., Serafimovich, A., Bargsten, A., Behrendt, T., Biermann, T., Breuninger, C., Dix, S., Gerken, T., Hunner, M., Lehmann-Pape, L., Hens, K., Jocher, G., Kesselmeier, J., Lüers, J., Mayer, J.-C., Moravek, A., Plake, D., Riederer, M., Rütz, F., Scheibe, M., Siebicke, L., Sörgel, M., Staudt, K., Trebs, I., Tsokankunku, A., Welling, M., Wolff, V., Zhu, Z., 2012. Coupling processes and exchange of energy and reactive and non-reactive trace gases at a forest site—results of the EGER experiment. Atmos. Chem. Phys. 12, 1923–1950.

Foken, T., 2008. Micrometeorology. Springer, Berlin/Heidelberg, pp. 308.

Fröhlich, N.J., Schmid, H.P., 2006. Flow divergence and density flows above and below a deciduous forest Part II. Below-canopy thermotopographic flows. Agric. For. Meteorol. 138, 29–43.

Fratini, G., Mauder, M., 2014. Towards a consistent eddy-covariance processing: an intercomparison of EddyPro and TK3. Atmos. Meas. Technol. 7, 2273–2281.

Galperin, B., Sukoriansky, S., Anderson, P.S., 2007. On the critical Richardson number in stably stratified turbulence. Atmos. Sci. Lett. 8, 65–69.

Goulden, M.L., Munger, J.W., Fan, S.-N., Daube, B.C., Wofsy, S.C., 1996. Measurements of carbon sequestration by long-term eddy covariance: methods and a critical evaluation of accuracy. Global Change Biol. 2, 169–182.

Goulden, M.L., Wofsy, S.C., Harden, J.W., Trumbore, S.E., Crill, P.M., Gower, S.T., Fries, T., Daube, B.C., Fan, S.-M., Sutton, D.J., Bazzaz, A., Munger, J.W., 1998. Sensitivity of boreal forest carbon balance to soil thaw. Science 279, 214–216.

Haei, M., Laudon, H., 2015. Carbon dynamics and changing winter conditions: a review of current understanding and future research directions. Biogeosci. Discuss. 12, 15763––15808.

Hasselquist, N.J., Metcalfe, D.B., Högberg, P., 2012. Contrasting effects of low and high nitrogen additions on soil CO_2 flux components and ectomycorrhizal fungal sporocarp production in a boreal forest. Global Change Biol. 18, 3596–3605.

IPCC. Climate Change 2014: Synthesis Report. Contribution of Working Groups I, II 751 and III to the Fifth Assessment Report of the Intergovernmental Panel on Climate Change 752 [Core Writing Team, Pachauri, R.K., Meyer, L.A., (Eds.)]. 2014, IPCC, Geneva, Switzerland, 151.

Ilvesniemi, H., Kähkönen, M.A., Pumpanen, J., Rannik, Ü., Wittmann, C., Perämäki, M., Keronen, P., Hari, P., Vesala, T., Salkinoja-Salonen, M., 2005. Wintertime CO_2 evolution from a boreal forest ecosystem. Boreal Environ. Res. 10, 401–408.

Keenan, T.F., Hollinger, D.Y., Bohrer, G., Dragoni, D., Munger, J.W., Schmid, H.P., Richardson, A.D., 2013. Increase in forest water-use efficiency as atmospheric carbon dioxide concentrations rise. Nature 499, 324–327.

Kolari, P., Pumpanen, J., Rannik, Ü., Ilvesniemi, H., Hari, P., Berninger, F., 2004. Carbon balance of different aged Scots pine forests in Southern Finland. Global Change Biol. 10, 1106–1119.
Kolari, P., Lappalainen, H.K., Hänninen, H., Hari, P., 2007. Relationship between temperature and the seasonal course of photosynthesis in Scots pine at northern timberline and in southern boreal zone. Tellus B 59, 542–552.
Kolari, P., Kulmala, L., Pumpanen, J., Launiainen, S., Ilvesniemi, H., Hari, P., Nikinmaa, E., 2009. CO_2 exchange and component CO_2 fluxes of a boreal Scots pine forest. Boreal Environ. Res. 14, 761–783.
Kutsch, W.L., Kolari, P., 2015. Data quality and the role of nutrients in forest carbon-use efficiency. Nat. Clim. Change 5, 959–960.
Laudon, H., Ottosson Löfvenius, M., 2016. Adding snow to the picture—providing complementary winter precipitation data to the Krycklan catchment study database. Hydrol. Processes, http://dx.doi.org/10.1002/hyp.10753.
Laudon, H., Taberman, I., Ågren, A., Futter, M., Ottosson Löfvenius, M., Bishop, K., 2013. The Krycklan catchment study—a flagship infrastructure for hydrology, biogeochemistry and climate research in the boreal landscape. Water Resour. Res. 49, 7154–7158.
Launiainen, S., Rinne, J., Pumpanen, J., Kulmala, L., Kolari, P., Keronen, P., Siivola, E., Pohja, T., Hari, P., Vesala, T., 2005. Eddy-covariance measurements of CO_2 and sensible and latent heat fluxes during a full year in a boreal pine forest trunk-space. Boreal Environ. Res. 10, 569–588.
Launiainen, S., Vesala, T., Mölder, M., Mammarella, I., Smolander, S., Rannik, Ü., Kolari, P., Hari, P., Lindroth, A., Katul, G.G., 2007. Vertical variability and effect of stability on turbulence characteristics down to the floor of a pine forest. Tellus B 59, 919–936.
Lee, X., Massmann, W.J., Law, B. (Eds.), 2004. Handbook of Micrometeorology: A Guide for Surface Flux Measurements and Analysis. Kluwer, Dordrecht, p. 250.
Lee, X., 2000. Air motion within and above forest vegetation in non-ideal conditions. For. Ecol. Manag. 135, 3–18.
Lim, H., Oren, R., Palmroth, S., Tor-ngern, P., Mörling, T., Näsholm, T., Lundmark, T., Helmisaari, H.-S., Leppälammi-Kujansuu, J., Linder, S., 2015. Inter-annual variability of precipitation constrains the production response of boreal *Pinus sylvestris* to nitrogen fertilization. For. Ecol. Manag. 348, 31–45.
Linder, S., Lohammar, T., 1981. Amount and quality of information on CO_2-exchange required for estimating annual carbon balance of coniferous trees. Stud. For. Suec. 160, 73–87.
Lindroth, A., Grelle, A., Moren, A.-S., 1998. Long-term measurements of boreal forest carbon balance reveal large temperature sensitivity. Global Change Biol. 4, 443–450.
Luyssaert, S., Inglima, I., Jung, M., Richardson, A.D., Reichstein, M., Papale, D., Piao, S.L., Schulze, E.-D., Wingate, L., Mateucchi, G., Aragao, L., Aubinet, M., Beer, C., Bernhofer, C., Black, K.G., Bonal, D., Bonnefond, J.-M., Chambers, J., Ciais, P., Cook, B., Davis, K.J., Dolman, A.J., Gielen, B., Goulden, M., Grace, J., Granier, A., Grelle, A., Griffis, T., Grünwald, T., Guidolotti, G., Hanson, P.J., Harding, R., Hollinger, D.Y., Hutyra, L.R., Kolari, P., Kruijt, B., Kutsch, W., Lagergren, F., Laurila, T., Law, B.E., Le Maire, G., Lindroth, A., Loustau, D., Malhi, Y., Mateus, J., Migliavacca, M., Misson, L., Montagnani, L., Moncrieff, J., Moors, E., Munger, J.W., Nikinmaa, E., Ollinger, S.V., Pita, G., Rebmann, C., Roupsard, O., Saigusa, N., Sanz, M.J., Seufert, G., Sierra, C., Smith, M.-L., Tang, J., Valentini, R., Vesala, T., Janssens, I.A., 2007. CO_2 balance of boreal, temperate, and tropical forests derived from a global database. Global Change Biol. 13, 2509–2537.
Mäkelä, A., Kolari, P., Karimäki, J., Nikinmaa, E., Perämäki, M., Hari, P., 2006. Modelling five years of weather-driven variation of GPP in a boreal forest. Agric. For. Meteorol. 139, 382–398.
Mahecha, M.D., Reichstein, M., Carvalhais, N., Lasslop, G., Lange, H., Seneviratne, S.I., Vargas, R., Ammann, C., Altaf Arain, M., Cescatti, A., Janssens, I.A., Migliavacca, M., Montagnani, L., Richardson, A.D., 2010. Global convergence in the temperature sensitivity of respiration at ecosystem level. Science 329, 838–840.
Markkanen, T., Rannik, Ü., Keronen, P., Suni, T., Vesala, T., 2001. Eddy covariance fluxes over a boreal Scots pine forest. Boreal Environ. Res. 6, 65–78.
Mauder, M., Foken, T., 2015. Eddy-Covariance Software TK3. Zendo, http://dx.doi.org/10.5281/zenodo.20349, 834.
McCallum, I., Franklin, O., Moltchanova, E., Merbold, L., Schmullius, C., Shvidenko, A., Schepaschenko, D., Fritz, S., 2013. Improved light and temperature responses for light-use-efficiency-based GPP models. Biogeosciences 10, 6577–6590.
Meyer, A., Tarvainen, L., Nousratpour, A., Björk, R.G., Ernfors, M., Grelle, A., Kasimir Klemedtsson, Å., Lindroth, A., Räntfors, M., Rütting, T., Wallin, G., Weslien, P., Klemedtsson, L., 2013. A fertile peatland forest does not constitute a major greenhouse gas sink. Biogeoscience 10, 7739–7758.
Misson, L., Baldocchi, D.D., Black, T.A., Blanken, P.D., Brunet, Y., Curiel Yuste, J., Dorsey, J.R., Falk, M., Granier, A., Irvine, M.R., Jarosz, N., Lamaud, E., Launiainen, S., Law, B.E., Longdoz, B., Loustau, D., McKay, M., U. Paw, K.T., Vesala, T., Vickers, D., Wilson, K.B., Goldstein, A.H., 2007. Partitioning forest carbon fluxes with overstory and understory eddy-covariance measurements: a synthesis based on FLUXNET data. Agric. For. Meteorol. 144, 14–31.
Morgenstern, K., Black, T.A., Humphreys, E.R., Griffis, T.J., Drewitt, G.B., Cai, T., Nesic, Z., Spittlehouse, D.L., Livingston, N.J., 2004. Sensitivity and uncertainty of the carbon balance of a Pacific Northwest Douglas-fir forest during an El Niño/La Niña cycle. Agric. For. Meteorol. 123, 201–219.
Oliveira, P.E.S., Acevedo, O.C., Moraes, O.L.L., Zimermann, H.R., Teichrieb, C., 2013. Nocturnal intermittent coupling between the interior of a pine forest and the air above it. Boundary Layer Meteorol. 146, 45–64.
Peichl, M., Brodeur, J.J., Khomik, M., Arain, M.A., 2010. Biometric and eddy-covariance based estimates of carbon fluxes in an age-sequence of temperate pine forests. Agric. For. Meteorol. 150, 952–965.
Poggi, D., Katul, G.G., Albertson, J.D., 2004. Momentum transfer and turbulent kinetic energy budgets within a dense model canopy. Boundary Layer Meteorol. 111, 589–614.
Rannik, Ü., Aubinet, M., Kurbanmuradov, O., Sabelfeld, K.K., Markkanen, T., Vesala, T., 2000. Footprint analysis for measurements over a heterogeneous forest. Boundary Layer Meteorol. 97, 137–166.
Rannik, Ü., Markkanen, T., Raittila, J., Hari, P., Vesala, T., 2003. Turbulence statistics inside and over forest: influence on footprint prediction. Boundary Layer Meteorol. 109, 163–189.
Raupach, M.R., Thom, A.S., 1981. Turbulence in and above plant canopies. Ann. Rev. Fluid Mech. 13, 97–129.
Ross, A.N., Grant, E.R., 2015. A new continuous planar fit method for calculating fluxes in complex, forested terrain. Atmos. Sci. Lett. 16, 445–452.
Schwalm, C.R., Williams, C.A., Schaefer, K., Arneth, A., Bonal, D., Buchmann, N., Chen, J., Law, B.E., Lindroth, A., Luyssaert, S., Reichstein, M., Richardson, A.D., 2010. Assimilation exceeds respiration sensitivity to drought: a FLUXNET synthesis. Global Change Biol. 16, 657–670.
Seok, B., Helmig, D., Williams, M.W., Liptzin, D., Chowanski, K., Hueber, J., 2009. An automated system for continuous measurements of trace gas fluxes through snow: an evaluation of the gas diffusion method at a subalpine forest site Niwot Ridge, Colorado. Biogeochemistry 95, 95–113.
Serafimovich, A., Thomas, C., Foken, T., 2011. Vertical and horizontal transport of energy and matter by coherent motions in a tall spruce canopy. Boundary Layer Meteorol. 140, 429–451.
Sommerfeld, R.A., Mosier, A.R., Musselman, R.C., 1993. CO_2, CH_4 and N_2O flux through a wyoming snowpack and implications for global budgets. Nature 361, 140–142.
Speckman, H.N., Frank, J.N., Bradford, J.B., Miles, B.L., Massman, W.J., Parton, W.J., Ryan, M.G., 2015. Forest ecosystem respiration estimated from eddy covariance and chamber measurements under high turbulence and substantial tree mortality from bark beetles. Global Change Biol. 21, 708–721.
Staebler, R.M., Fitzjarrald, D.R., 2004. Observing subcanopy CO_2 advection. Agric. For. Meteorol. 122, 139–156.
Staebler, R.M., Fitzjarrald, D.R., 2005. Measuring canopy structure and the kinematics of subcanopy flows in two forests. J. Appl. Meteorol. 44, 1161–1179.
Strand, M., Öquist, G., 1985. Inhibition of photosynthesis by freezing temperatures and high light levels in cold-acclimated seedlings of Scots pine (Pinus sylvestris). – I. Effects on the light-limited and light-saturated rates of CO_2 assimilation. Physiol. Plant. 64, 425–430.
Stull, R.B., 1988. An Introduction to Boundary Layer Meteorology. Kluwer Acad. Publ., Dordrecht, Boston, London, pp. 666.
Suni, T., Rinne, J., Reissell, A., Altimir, N., Keronen, P., Rannik, Ü., Dal Maso, M., Kulmala, M., Vesala, T., 2003. Long-term measurements of surface fluxes above a Scots pine forest in Hyytiälä southern Finland 1996–2001. Boreal Environ. Res. 8, 287–301.
Thomas, C., Foken, T., 2007. Flux contributions of coherent structures and its implications for the exchange of energy and matter in a tall spruce canopy. Boundary Layer Meteorol. 123, 317–337.
Thomas, C.K., Martin, J.G., Law, B.E., Davis, K., 2013. Toward biologically meaningful net carbon exchange estimates for tall, dense canopies: multi-level eddy covariance observations and canopy coupling regimes in a mature Douglas-fir forest in Oregon. Agric. For. Meteorol. 173, 14–27.
Troeng, E., Linder, S., 1982. Gas exchange in a 20-year-old stand of Scots pine. I. Net photosynthesis of current and one-year-old shoots within and between seasons. Physiol. Plant. 54, 7–14.
Vickers, D., Irvine, J., Martin, J.G., Law, B.E., 2012. Nocturnal subcanopy flow regimes and missing carbon dioxide. Agric. For. Meteorol. 152, 101–108.
Winston, G.C., Sundquist, E.T., Stephens, B.B., Trumbore, S.E., 1997. Winter CO_2 fluxes in a boreal forest. J. Geophys. Res. D: Atmos. 102, 28795–28804.
Zha, T., Xing, Z., Wang, K.-Y., Kellomäki, S., Barr, A.G., 2007. Total and component carbon fluxes of a Scots pine ecosystem from chamber measurements and eddy covariance. Ann. Bot. 99, 345–353.
Zhao, J., Peichl, M., Öquist, M.G., Nilsson, M.B., 2016. Gross primary production controls the subsequent winter CO_2 exchange in a boreal peatland. Global Change Biol., http://dx.doi.org/10.1111/gcb.13308, early view.